

GEOACOUSTIC INVERSION WITH STRONGLY CORRELATED DATA ERRORS

Jan Dettmer¹, Stan E. Dosso¹, and Charles W. Holland²

¹School of Earth and Ocean Sciences, University of Victoria, BC, Canada jand@uvic.ca

²Applied Research Laboratory, The Pennsylvania State University, State College, PA, USA

1. INTRODUCTION

Geoacoustic inversion infers seabed properties from acoustic measurements in the water column. A typical assumption in geoacoustic inversion is that the data errors are uncorrelated and obey certain statistics, e.g., are Gaussian distributed. However, real data often show strong error correlations. In the past, this has been dealt with by sub-sampling the data to a point where correlations disappear. However, sub-sampling the data is always a trade off between reducing correlations and losing information.

This paper considers pre-processing of synthetic single bounce reflection-loss data with strongly correlated data errors to improve application of a nonlinear Bayesian inversion to recover geoacoustic parameters from a viscoelastic model. Correlated Gaussian errors are generated using a realistic synthetic covariance matrix derived from experimental measurements [1]. The inverse problem is solved with fast Gibbs sampling [2], which provides parameter estimates and credibility intervals by sampling the posterior probability density. The error correlations are taken into account by estimating a covariance matrix from the data residuals obtained from a solution to the inverse problem. This covariance matrix is then used in the cost function of the fast Gibbs sampler. The recovered covariance matrix is compared to the original and stringent statistical tests are applied to the data residuals to illustrate the benefits of this rigorous error treatment. The geoacoustic parameters of the viscoelastic model are clearly resolvable and show reasonable error bounds for correlated errors.

2. Method

The pre-processing of fast Gibbs sampling [2] to apply it to synthetic data with correlated data errors involves three basic steps. First, zero mean Gaussian noise n'_i of standard deviation 1 is generated for each frequency f_i . In a second step, the noise is then correlated using a covariance matrix for each frequency $C^{(d_i)}$. This can be done by forming the Cholesky decomposition of the matrix

$$(1) \quad C^{(d_i)} = LL^T,$$

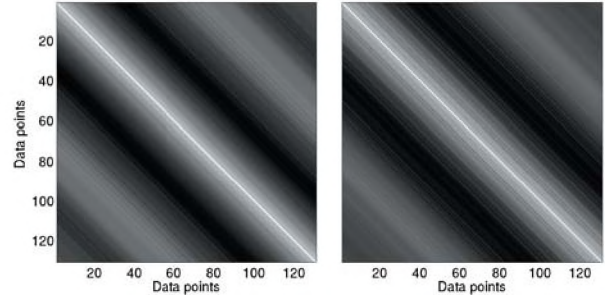


Fig. 1. Original (left) and recovered (right) covariance matrices for 1600 Hz.

where L is the lower triangular matrix. Then, calculating

$$(2) \quad n_i = Ln'_i$$

gives noise that is drawn from a Gaussian distribution with respect to the data covariance matrices $C^{(d_i)}$ at each frequency. The noise is then added to the synthetic data that were computed with a forward model that calculates the plane wave response of the sub-bottom as a function of frequency and angle.

To recover $C^{(d_i)}$, residuals \tilde{n}_i are calculated from predicted and real data. The predicted data are calculated from a maximum likelihood model that is found by applying global optimization to determine the geoacoustic model parameters which best fit the noisy data. The autocovariance can then be calculated as a function of \tilde{n}_i . Theoretically, the covariance should be calculated as an ensemble average. In reality, however, we have access to only a single finite subset of the random process. By assuming an ergodic process, we replace the ensemble average by an average over angles, and the j^{th} element of the autocovariance function for the finite subset \tilde{n}_i can be estimated as

$$(3) \quad c_j^{(d_i)} = \frac{1}{N_i} \sum_{k=0}^{N_i-j-1} n_i(k+j)n_i(k),$$

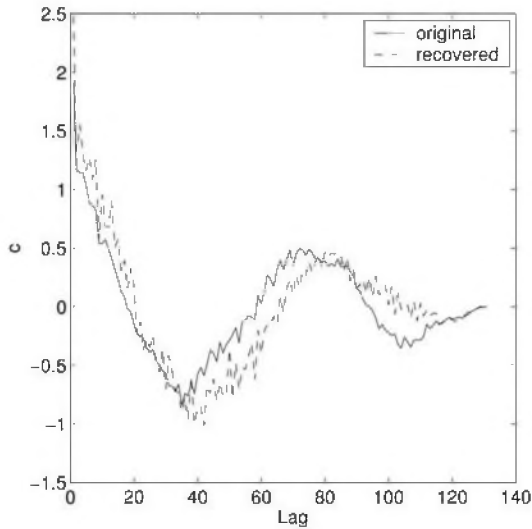


Fig. 2. First row of original covariance matrix and recovered covariance matrix after one iteration for a frequency of 1600 Hz.

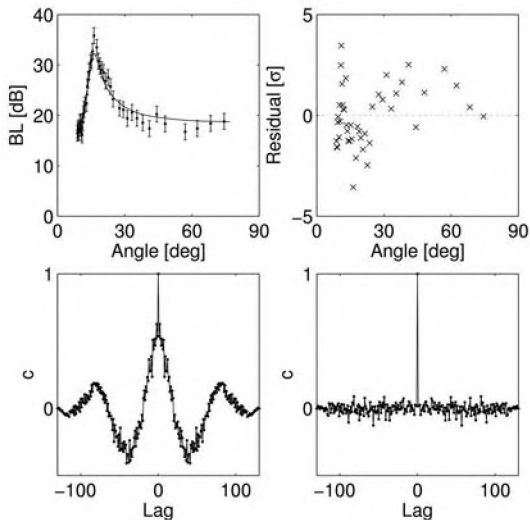


Fig. 3. (a) Fit of predicted data (solid line) and synthetic data with correlated errors and (b) the residuals that clearly show the correlations for 1600 Hz. (c) and (d) show the normalised autocovariance of the residuals with and without the recovered covariance matrix was taken into account, respectively.

where N_i is the number of angles at frequency f_i . Every term $c_j^{(d_i)}$ then builds one diagonal in the symmetric covariance matrix. The normalisation factor N_i does not strictly result in an average but rather damps terms in eq. (3) that do not have many samples to average over and hence have higher uncertainty. The covariance matrix estimate can be iteratively improved by using the estimates in subsequent global optimizations. The recovered covariance matrix can then be used in the Gibbs sampler by implementing the likelihood function L for multiple frequencies

$$(4) \quad L(m) \propto \prod_{i=1}^F \exp(-n_i^T (C^{(d_i)})^{-1} n_i),$$

where F is the number of frequencies and m is the model.

3. RESULTS

The data set used here contained 8 frequencies in a band from 300 to 1600 Hz with different numbers of angles at each frequency (between 54 and 131 data points at each frequency). For simplicity, the results are illustrated with only one frequency, 1600 Hz. The covariance matrices used here are taken from an analysis of real data collected in the Strait of Sicily [1] that showed strongly correlated errors.

Fig. 2 compares the original and the recovered covariance matrix after one iteration for 1600 Hz. It can be seen that there is a close match between the two. Inversion results (not shown here) with the two matrices show that both the recovered models and the parameter uncertainty bounds are very close as well.

Fig. 3 (a) and (b) show the fit of the predicted data to the synthetic data, and the residuals. It is obvious that the data have strong correlations. Fig. 3 also shows the auto covariance function for the data residuals and for residuals to which the Cholesky decomposition of the recovered covariance matrix was applied by

$$(5) \quad \tilde{n}_i = L^{-1} n_i.$$

These two plots indicate that the recovered covariance matrix is capable to take all important correlations into account. To statistically quantify the effect of using $C^{(d_i)}$, a

runs test was performed. The data residuals n_i strongly fail the runs test ($p < 0.001$), whereas the data residuals \tilde{n}_i easily pass the tests ($p = 0.39$). In the inversion, the geoacoustic parameters show more realistic uncertainty bounds if $C^{(d_i)}$ is used in the energy function. It is thus important to correctly treat error correlations if reasonable uncertainties are to be estimated from the data.

REFERENCES

- [1] C. W. Holland and J. Osler. High-resolution geoacoustic inversion in shallow water: A joint time- and frequency-domain technique. *J. Acoust. Soc. Am.*, 107, pp. 1263-1279. 2000.
- [2] S. E. Dosso. Quantifying uncertainty in Geoacoustic Inversion. I. A fast Gibbs sampler approach. *J. Acoust. Soc. Am.*, 111, pp. 129-142. 2002.